HIPPOCAMPUS 23:75–86 (2013)

Interaction of Inhibition and Triplets of Excitatory Spikes Modulates the NMDA-R-Mediated Synaptic Plasticity in a Computational Model of Spike Timing-Dependent Plasticity

Vassilis Cutsuridis*

ABSTRACT: Spike timing-dependent plasticity (STDP) experiments have shown that a synapse is strengthened when a presynaptic spike precedes a postsynaptic one and depressed vice versa. The canonical form of STDP has been shown to have an asymmetric shape with the peak long-term potentiation at +6 ms and the peak long-term depression at −5 ms. Experiments in hippocampal cultures with more complex stimuli such as triplets (one presynaptic spike combined with two postsynaptic spikes or one postsynaptic spike with two presynaptic spikes) have shown that pre–post–pre spike triplets result in no change in synaptic strength, whereas post–pre–post spike triplets lead to significant potentiation. The sign and magnitude of STDP have also been experimentally hypothesized to be modulated by inhibition. Recently, a computational study showed that the asymmetrical form of STDP in the CA1 pyramidal cell dendrite when two spikes interact switches to a symmetrical one in the presence of inhibition under certain conditions. In the present study, I investigate computationally how inhibition modulates STDP in the CA1 pyramidal neuron dendrite when it is driven by triplets. The model uses calcium as the postsynaptic signaling agent for STDP and is shown to be consistent with the experimental triplet observations in the absence of inhibition: simulated pre–post–pre spike triplets result in no change in synaptic strength, whereas simulated post–pre–post spike triplets lead to significant potentiation. When inhibition is bounded by the onset and offset of the triplet stimulation, then the strength of the synapse is decreased as the strength of inhibition increases. When inhibition arrives either few milliseconds before or at the onset of the last spike in the pre–post–pre triplet stimulation, then the synapse is potentiated. Variability in the frequency of inhibition (50 vs. 100 Hz) produces no change in synaptic strength. Finally, a 5% variation in model's calcium parameters (calcium thresholds) proves that the model's performance is robust. © 2012 Wiley Periodicals, Inc.

KEY WORDS: computational model; STDP; calcium; NMDA; inhibition; hippocampus; CA1 pyramidal cell; triplets

INTRODUCTION

In 1949, Hebb stated that coincident firing of inputs onto a neuron or coincident firing of presynaptic and postsynaptic neurons strengthens synaptic connections. The cellular correlates of this associative learning law were later found to be the long-term potentiation (LTP; Bliss and Lomo, 1970) and long-term depression (LTD; Stent, 1973). LTP is generally induced by short, high-frequency stimulation (HFS), whereas LTD is generally induced by prolonged low-frequency stimulation (Dunwiddie and Lynch, 1978). Typical frequencies used to induce HFS–LTP are in the range of 10–250 Hz and contain 20–100 stimuli with trains of stimuli presented multiple times (Dunwiddie and Lynch, 1978). For LTD induction, frequencies range from 1 to 3 Hz, and the number of stimuli is 100–900 (Dunwiddie and Lynch, 1978; Dudek and Bear, 1993).

Although effective, HFS does not resemble any physiological patterns of activity. Patterned stimulation resembling physiological activity is the theta burst stimulation, which has been shown to be effective for LTP induction (Larson et al., 1986). Theta burst stimulation consists of short bursts (4–5 stimuli at 100 Hz) repeated at 5 Hz, which lies within the hippocampal theta frequency range (4–12 Hz; Bland, 1986; Buzsáki, 2002). Primed burst stimulation, another form of patterned stimulation, involves delivery of a priming stimulus followed by a single short burst (Larson and Lynch, 1986; Rose and Dunwiddie, 1986). Primed burst LTP is induced in intervals ranging from 140 to 200 ms (Larson and Lynch, 1986, 1989). Intervals less than 140 ms or greater than 200 ms have been shown to be ineffective. Recently, burst stimulation at frequencies ranging from 2 to 3.5 Hz induced maximal LTP at Schaffer collateral CA1 synapses (Grover et al., 2009). Theta burst stimulation has also been used in urethane-anesthetized animals (Pavlides et al., 1988) and in awake-behaving animals (Hyman et al., 2003).

It is currently accepted that the critical component for the induction of long-term synaptic change is an increase in intracellular Ca^{2+} concentration in the postsynaptic dendrite with the magnitude and duration of Ca^{2+} increase determining the direction of plasticity (Bear et al., 1987; Lisman, 1989; Hansel et al., 1996). It was proposed that short, large magnitude increases in intracellular Ca^{2+} concentration lead to synaptic potentiation, whereas prolonged, small magnitude increases lead to synaptic depression (Cho et al., 2001; Ismailov et al., 2004; Gall et al., 2005; Hansel et al., 1997).

The increase in intracellular Ca^{2+} is due to a number of different sources including voltage-dependent Ca^{2+} channels, intracellular Ca^{2+} stores, and through NMDA receptors. An NMDA receptor opens and allows Ca^{2+} to flow in only when presynaptic glutamate release is coincident with postsynaptic depolarization causing the removal of voltage-dependent magne-

Division of Engineering, King's College London, United Kingdom
Additional Supporting Information may be found in the online version of this article.
*Correspondence to: Division of Engineering, King's College London, UK. E-mail: vcutsuridis@gmail.com
Accepted for publication 5 July 2012
DOI 10.1002/hipo.22057
Published online 31 July 2012 in Wiley Online Library (wileyonlinelibrary.com).

sium block inside the NMDA channel pore (Mayer et al., 1984; Nowak et al., 1984). Strong activation of the NMDA receptor leading to a large Ca^{2+} influx at the postsynaptic site induces LTP, whereas weak NMDA receptor activation and moderate Ca^{2+} influx result in LTD (Bliss and Collingdridge, 1993).

Recently, it has been shown that the temporal precision of the presynaptic and postsynaptic action potentials (APs) is critical. If the presynaptic AP occurred before the postsynaptic AP, then LTP is induced, but when the timings are reversed, LTD is induced (Bell et al., 1997; Magee and Johnston, 1997; Markram et al., 1997; Bi and Poo, 1998; Debanne et al., 1998; Nishiyama et al., 2000). This phenomenon has been termed spike-timing dependent plasticity (STDP) and has been demonstrated in a number of brain areas and across species both in vivo and in vitro (Bi and Poo, 1998; Debanne et al., 1998; Zhang et al., 1998; Feldman, 2000; Sjostrom et al., 2001; Froemke and Dan, 2002; Tzounopoulos et al., 2004; Bender et al., 2006; Cassenaer and Laurent, 2007). However, experiments with pairs of spikes do not necessarily mean that the spike pairs are more important than three spikes (triplets) and four spikes (quadruplets).

Recent experiments (Froemke and Dan, 2002; Wang et al., 2005; Froemke et al., 2006) have investigated STDP triggered by spike triplets (one presynaptic spike combined with two postsynaptic spikes or one postsynaptic spike with two presynaptic spikes) and spike quadruplets (a pair of pre- and postsynaptic spikes followed by another pair of post- and presynaptic spikes or a pair of post- and presynaptic spikes followed by another pair of pre- and postsynaptic spikes). It was shown in hippocampal cultures that pre–post–pre spike triplets result in no change in synaptic strength, whereas post–pre–post spike triplets lead to significant potentiation (Wang et al., 2005). This result was shown to be partially consistent with the findings in visual cortical slices (Sjostrom et al., 2001).

Another set of experiments have shown that the STDP observed asymmetry when two spikes pair can sometimes change with the target and the location of the synapse (Tzounopoulos et al., 2004; Froemke et al., 2005; Letzkus et al., 2006; Caporale and Dan, 2009) and can be dynamically regulated by the activity of adjacent synapses (Harvey and Svoboda, 2007; Caporale and Dan, 2009), presynaptic GABA inhibition (Tsukada et al., 2005; Aihara et al., 2007), or by the action of neuromodulators (Seol et al., 2007; Caporale and Dan, 2009). Optical imaging studies (Tsukada et al., 2005; Aihara et al., 2007) in the hippocampus suggested that the asymmetry-to-symmetry transition of the STDP profile in the CA1 pyramidal cell dendrites might be due to inhibition, but they failed to specify the inhibitory conditions under which such a transition is possible.

In the hippocampus, inhibition comes in various frequencies (theta, gamma, and ripples) and different phases with the ongoing network oscillations and inhibits distinct subcellular domains of pyramidal cells (PCs; Gloveli et al., 2010; references therein). Axo-axonic (AACs) cells innervate exclusively the axon initial segment of PCs, whereas basket cells (BCs) innervate the somata and proximal apical dendrites. OLM cells innervate the distal PC dendrites, whereas the bistratified (BSC), trilaminar, and radiatum cells innervate the proximal and oblique PC dendrites. In CA1, during sharp wave ripple oscillations, BCs and BSCs strongly increase their discharge rates in phase with the ripple episode (Klausberger and Somogyi, 2008). In contrast, AACs fire before the ripple episode, but pause their activities during and after it. OLM cells pause their firings during ripples. On the other hand, during theta oscillations, OLM cells, BSCs, and PCs increase their firing rates at the troughs of the extracellular theta, whereas BCs and AACs fire at the peaks of it. During gamma oscillations, the firing rates of BCs, AACs, and BSCs correlate with the extracellular gamma in different degrees, whereas OLM cells do not correlate with gamma oscillations.

Inhibitory interneurons entrain excitatory cells to fire at different frequencies. BCs have been shown to phase spontaneous firing and subthreshold oscillations in CA1 pyramidal cells at theta frequencies (Cobb et al., 1995), whereas OLM cells constitute an intrahippocampal mechanism for pacing nested gamma–theta rhythms in CA1 and CA3 regions (White et al., 2000). Networks of inhibitory interneurons have been shown to entrain hippocampal pyramidal cells at 40 Hz (Whittington et al., 1995). During gamma oscillations in vivo and in vitro, the different classes of interneurons fire APs at different phases with respect to the external oscillation and the firing of the pyramidal cells (Gloveli et al., 2010).

Cutsuridis (2011) was the first to computationally show in a quantitative way the inhibitory conditions under which this asymmetry-to-symmetry transition is possible in the CA1 pyramidal cell stratum radiatum (SR) dendrites. The model predicted that (1) inhibition is the necessary factor for the asymmetry-to-symmetry switch in the STDP form as suggested by experimentalists (Nishiyama et al., 2000; Tsukada et al., 2005; Aihara et al., 2007), (2) a theta-modulated inhibitory spike has no effect on the asymmetrical form, sign, and magnitude of STDP, (3) a theta-modulated inhibitory burst is the necessary condition for the asymmetry-to-symmetry transition in the pyramidal cell dendrite, (4) the transition strongly depends on the strength inhibition and its relative onset with respect to excitatory stimulation, and (5) variability in the frequency of the inhibitory burst produces no differential effect in the sign, magnitude, and form of STDP in the pyramidal cell dendrite. Experimental studies (Klausberger et al., 2003; 2004; Klausberger and Somogyi, 2008; Klausberger, 2009) have shown that the firing activities of most inhibitory cells in region CA1 are phasic (bursting), oscillatory (repeated every theta cycle), and present at various phases of the field theta and the activity of pyramidal cells. OLM cells tend to fire right after the pyramidal cells, which resembles the Cutsuridis (2011) simulated pattern (doublets preceding the inhibitory burst). BSC cells firing partially overlap with the firing of pyramidal cells, much like in the Cutsuridis's (2011) computational study where inhibition precedes and partially overlaps with the doublet excitatory pattern. Inhibition repeats in every theta cycle as in the Cutsuridis's (2011) study.

In contrast to the Cutsuridis's study (2011) where a pair of pulse stimuli was used to study how the form of STDP profile changes in the presence of inhibition, the scope of this work is to understand how spike timing-dependent synaptic plasticity is

induced by triplets and how this plasticity is affected when inhibition is present. The model's performance is initially validated against the Wang et al.'s (2005) experimental data (see Fig. 3). Then, STDP is tested against the strength, frequency, and timing of inhibition with respect to the excitatory pre–post–pre or post–pre–post triplet stimulation. Excitatory and inhibitory theta-modulated inputs drive the soma and dendrite of a CA1 pyramidal cell model. Plasticity effects in the dendrite are measured via a biophysical mechanism based on a calcium detector system, which respond not only to calcium level (Abarbanel et al., 2002; Karmarkar and Buonomano, 2002; Shouval et al., 2002) but also to Ca^{2+} temporal dynamics in the dendrite (Sabatini et al., 2001; Ismailov et al., 2004). This calcium detector system has been shown to yield a number of empirical findings from multispike experiments (e.g., pre–post LTP, post–pre LTD without a pre–post LTD window; Rubin et al., 2005; Cutsuridis, 2011). The CA1 pyramidal cell model leads to a number of experimentally testable predictions that may lead to a better understanding of the STDP in the CA1 pyramidal cells of the hippocampus.

MATERIALS AND METHODS

The CA1 Pyramidal Cell Model

The model CA1 pyramidal cell (see Fig. 1A) consists of two compartments: a soma and a dendrite. The somatic compartment contains a sodium (Na^+) current, a delayed rectifier K^+ current, an A-type K^+ current, a calcium-activated after-hyperpolarizing (AHP) K^+ current, and a HVA L-type Ca^{2+} current. The dendritic compartment contains a sodium (Na^+) current, a delayed rectifier K^+ current, an A-type K^+ current, and a HVA L-type Ca^{2+} current. AMPA, NMDA, and GABA-A synapses are present only in the dendrite.

In the model, calcium enters the neuron through (1) voltage-gated calcium channels (VGCCs) and (2) NMDA channels located at the dendrite. VGCCs are activated by the arrival of back-propagating action potentials (BPAPs) initiated in the soma by excitatory postsynaptic spikes. The NMDA channels are activated by the synergistic action of excitatory postsynaptic potentials and sufficient membrane potential depolarization due to the BPAP, which removes the magnesium block and allows calcium to enter the cell.

Plasticity is measured by a Ca^{2+} dynamics model (Rubin et al., 2005). The Ca^{2+} dynamics model consists of three biochemical detectors, which respond to the instantaneous calcium level and its time course in the dendrite and change the strength of the synapse accordingly (Fig. 1A). More specifically, the detection system consists of (1) a potentiation detector (P), which detects calcium levels above a high-threshold (4 μM) and triggers LTP, (2) a depression filter (D), which detects calcium levels that exceed a low-threshold level (0.6 μM), remain above it for a minimum time period, and trigger LTD, and (3) a veto detector (V), which detects levels exceeding a mid-level threshold (2 μM) and triggers a veto of the model's depression components.

The detailed mathematical formalism of the model and its detector system can be found in the Mathematical Formalism section (see Supporting Information). The parameters of all ionic and synaptic currents used in the model are listed in Table S1 (see Supporting Information). The parameters of the calcium detector system are listed in Table S2 (see Supporting Information).

Inputs

Two spike generators emulating the excitatory transient inputs to the soma and the dendrite were used to simulate the experimental STDP protocols. The presynaptic spike generator at the dendrite is given by

$$\begin{aligned}F_{\text{pre}}(t) = {} & H(t-1)\cdot(H(\sin(2\pi\cdot(t-2)/T))\\ & \cdot(1-H(\sin(2\pi\cdot(t-1)/T))))+\ ror\cdot H(t-1)\\ & \cdot(H(\sin(2\pi\cdot(t-2-\Delta\tau_1-\Delta\tau_2)/T))\cdot(1-H(\sin(2\pi\\ & \cdot(t-1-\Delta\tau_1-\Delta\tau_2)/T)))) \quad (1)\end{aligned}$$

where $\Delta\tau_1$ is the interval between the first presynaptic (dendritic) spike and the postsynaptic (somatic) spike, $\Delta\tau_2$ is the interval between the postsynaptic (somatic) spike and the second presynaptic (dendritic) spike, *ror* is a free parameter (1 when a presynaptic stimulation is followed by a postsynaptic one followed by a second presynaptic stimulation (pre–post–pre) and 0 otherwise), T is the period of oscillation, and $H(\ )$ is the Heaviside function. The postsynaptic spike generator at the soma is given by

$$\begin{aligned}F_{\text{post}}(t) = {} & H(t-1)\cdot(H(\sin(2\pi\cdot(t-2-\Delta\tau_1)/T))\\ & \cdot(1-H(\sin(2\pi\cdot(t-1-\Delta\tau_1)/T))))+\ oro\cdot H(t-1)\\ & \cdot(H(\sin(2\pi\cdot(t-2+\Delta\tau_2)/T))\\ & \cdot(1-H(\sin(2\pi\cdot(t-1+\Delta\tau_2)/T)))) \quad (2)\end{aligned}$$

where *oro* is a free parameter [1 when a postsynaptic stimulation is followed by a presynaptic one followed by a second postsynaptic stimulation (post–pre–post) and 0 otherwise]. In all experiments, a triplet was repeated every 300 ms typically for 5 s unless mentioned otherwise.

An inhibitory transient input to the dendrite was also used to investigate how inhibition modulates the NMDA-R-mediated STDP. The dendritic inhibitory spike generator is given by

$$F_{\text{GABA}}(t) = \sum_{i=1}^{N} F_{\text{GABA}_i}(t) \quad (3)$$

where

$$\begin{aligned}F_{\text{GABA}_i}(t) = {} & -ror\cdot aa_i\cdot H(t-1)\cdot(H(\sin(2\pi\\ & \cdot(t-2+\text{offset}-(i-1)\cdot\Delta\tau_{\text{GABA}})/T))\\ & \cdot(1-H(\sin(2\pi\cdot(t-1+\text{offset}-(i-1)\\ & \cdot\Delta\tau_{\text{GABA}})/T)))))-oro\cdot aa_i\cdot H(t-1)\\ & \cdot(H(\sin(2\pi\cdot(t-2+\text{offset}-\Delta\tau_i-(i-1)\cdot\Delta\tau_{\text{GABA}})/T))\\ & \cdot(1-H(\sin(2\pi\cdot(t-1+\text{offset}-\Delta\tau_i-(i-1)\\ & \cdot\Delta\tau_{\text{GABA}})/T)))))\end{aligned}$$

where *offset* is the relative timing between the onset of the GABA spike train and the pre–post interstimulus interval,

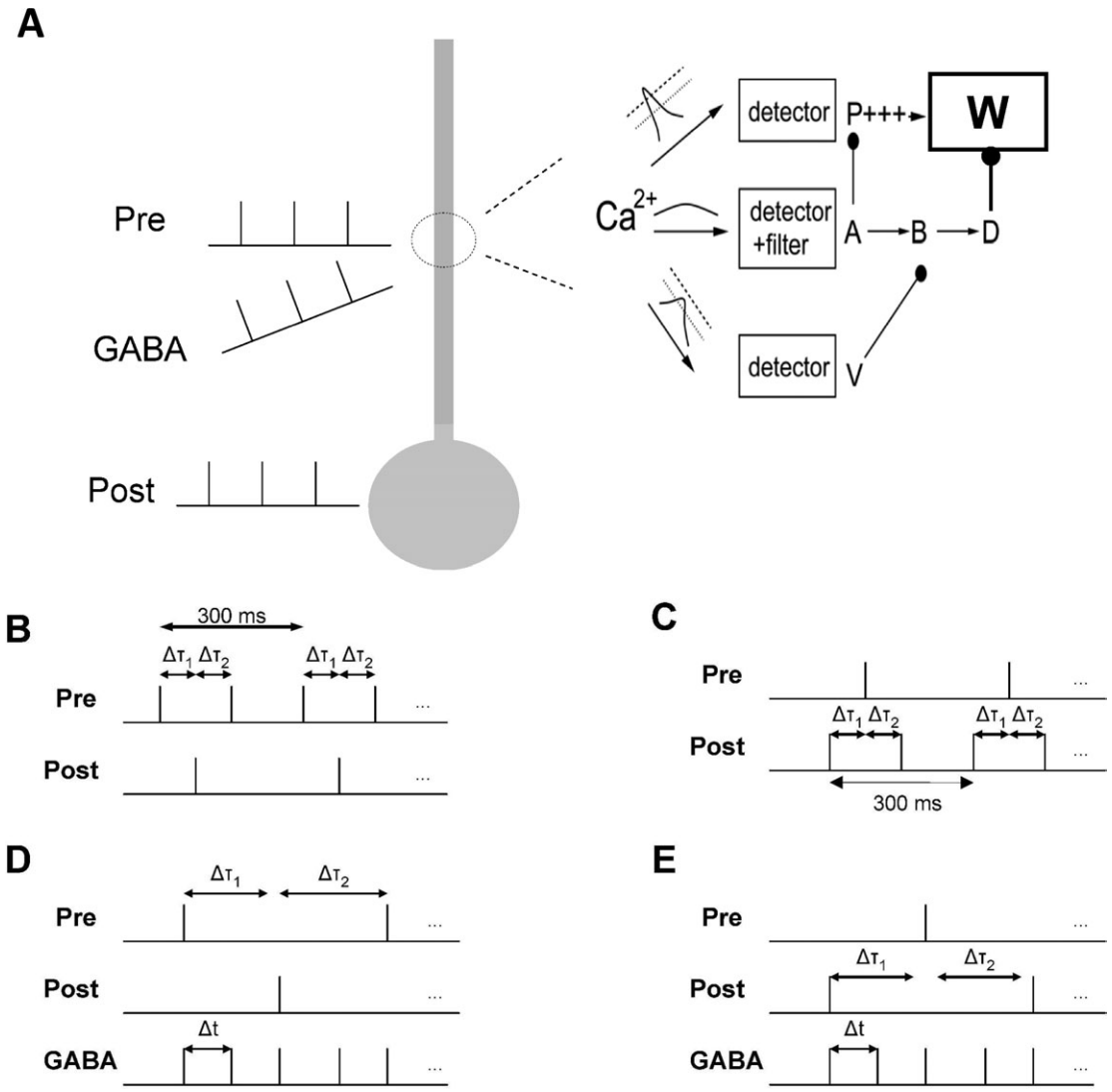

FIGURE 1. A: The model CA1 neuron with its three transient inputs to the soma and dendrite. Synaptic plasticity at the dendritic synapses (circled region) is computed by a model detector system that responds to $[Ca^{2+}]$ and produces an output of appropriate sign and magnitude. Three detector agents respond to the instantaneous $[Ca^{2+}]$ in the model dendrite. Different calcium time courses lead to different time courses of the detectors *P*, *V*, and *A*. An intermediate element B is activated by *A*, while an additional agent *D* is activated by *B*, which is suppressed or vetoed by *V*. *P* and *D* then compete to influence the plasticity variable *W*, which serves as a measure of sign and magnitude of synaptic strength changes from the baseline. *D* acts as a filter to map $[Ca^{2+}]$ time course onto *W*. B: Model triplet stimulation protocol consisting of a presynaptic dendritic stimulation followed by a postsynaptic somatic stimulation followed by a second presynaptic dendritic stimulation. $\Delta\tau_1$ was the interval between the postsynaptic spike and the first presynaptic spike, whereas $\Delta\tau_2$ was the interval between the second presynaptic spike and the postsynaptic one. The repetition period of each triplet was set to 300 ms. C: Model triplet stimulation protocol consisting of a postsynaptic somatic stimulation followed by a presynaptic dendritic stimulation followed by a second postsynaptic somatic stimulation. $\Delta\tau_1$ was the interval between the first postsynaptic spike and the presynaptic one, whereas $\Delta\tau_2$ was the interval between the second postsynaptic spike and the presynaptic one. The repetition period in this triplet protocol was set to 300 ms. D,E: Model triplet stimulation protocols (pre–post–pre and post–pre–post) in the presence of an inhibitory burst with interspike interval of 10 ms (100 Hz). Both inhibitory burst and triplet stimulation was repeated every 300 ms.

$\Delta\tau_{GABA}$ is the inhibitory burst interspike interval, and aa_i is either 1 or 0 depending on the duration of the interval between the presynaptic and the postsynaptic stimuli used.

Implementation

All simulations were performed using the software XPPAUT (Ermentrout, 2002). A fourth-order Runge–Kutta method was used for numerical integration in XPPAUT with a step size of $\delta t = 0.075$ ms. The MATLAB graphics toolbox was used for the visualization of the simulation results.

EXPERIMENTAL

A series of experiments in the presence of triplets with and without inhibition were performed, while varying the strength

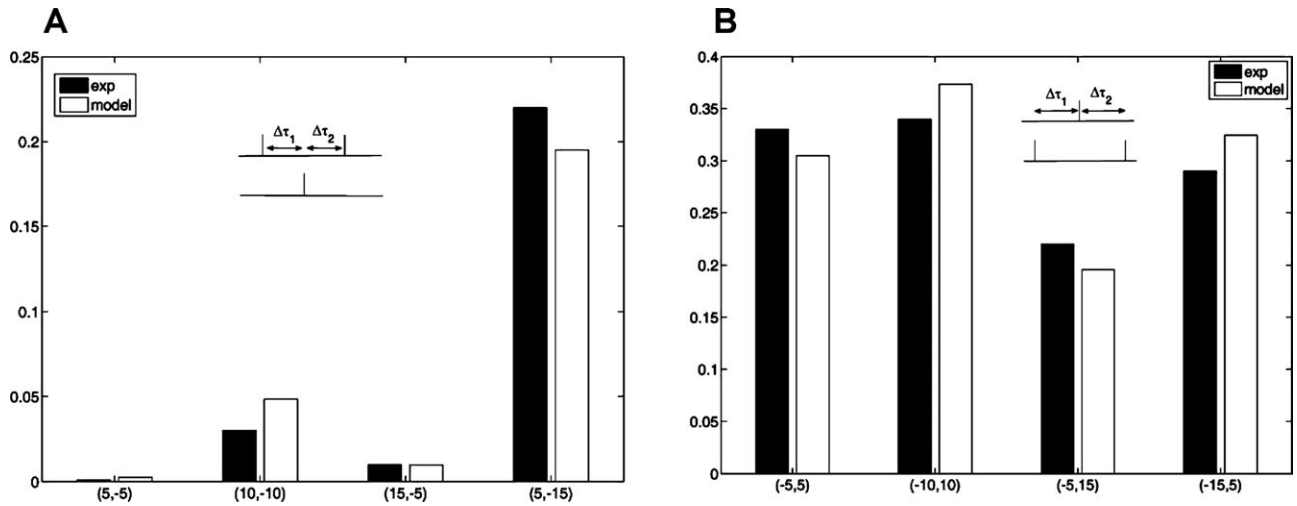

FIGURE 2. A: Comparison of experimental [Wang et al., 2005; see also Table 2 in Pfister and Gerstner (2006)] and simulated synaptic weight changes W_∞ for four different pre–post–pre triplet (pre-5-post-5-pre, pre-10-post-10-pre, pre-5-post-15-pre, and pre-15-post-5-pre) stimulation scenarios in the absence of inhibition. B: Comparison of experimental [Wang et al., 2005; see also Table 2 in Pfister and Gerstner (2006)] and simulated synaptic weight changes W_∞ for four different post–pre–post triplet stimulation scenarios (post-5-pre-5-post, post-10-pre-10-post, post-5-pre-15-post, and post-15-pre-5-post) in the absence of inhibition.

and frequency of inhibition and the relative timing between the inhibitory spike train and the triplet excitation and measured the calcium influx and subsequently the synaptic strength change at the dendrite. The same model (Cutsuridis, 2011) has been successful at replicating a series of experimental data when two excitatory spikes (doublet) were paired together in the presence and absence of inhibition (Bi and Poo, 1998; Tsukada et al., 2005; Aihara et al., 2007).

Model Validation: Triplets in the Absence of Inhibition

In cultured hippocampal neurons, triplet spiking with +10-ms pre–post spike timing and −10-ms post–pre spike timing (pre-10-post-10-pre) induces no significant synaptic strength change, whereas triplet spiking with −10 ms post–pre spike timing and +10-ms pre–post spike timing (post-10-pre-10-post) induces significant LTP (Wang et al., 2005). Similar results were obtained in experiments with spike timing ±5 ms (Wang et al., 2005). Triplet experiments with unequal spike timings (pre-15-post-5-pre, pre-5-post-15-pre, post-5-pre-15-post, and post-15-pre-5-post) resulted in three with significant potentiation (pre-5-post-15-pre, post-5-pre-15-post, and post-15-pre-5-post) and one with small synaptic change (pre-15-post-5-pre; Wang et al., 2005). Figure 2 shows a direct comparison of the Wang et al. (2005) experimentally observed synaptic strength change and the simulated one (W_∞) from all eight triplet stimulation paradigms. Each simulated pre–post–pre triplet paradigm (see Fig. 1B) consisted of 16 sets of three spikes repeated at 300 ms for about 5 s. Each pre–post–pre triplet consisted of two presynaptic dendritic spikes and one postsynaptic somatic spike characterized by $\Delta\tau_1 = t^{post} - t_1^{pre}$ and $\Delta\tau_2 = t_2^{pre} - t^{post}$ where t_1^{pre} and t_2^{pre} are the first and second presynaptic spikes of the triplet. Each simulated post–pre–post triplet paradigm (see Fig. 1C) consisted of 16 triplets repeated at 300 ms for about 5 s. In contrast to the previous protocol, in this one, a triplet consisted of one dendritic presynaptic and two somatic postsynaptic spikes. In this case, $\Delta\tau_1 = t_1^{post} - t^{pre}$ and $\Delta\tau_2 = t^{pre} - t_2^{post}$, where t_1^{post} and t_2^{post} are, respectively, the first and second postsynaptic spikes of the triplet. The synaptic strength value (W_∞) was recorded at the end of each simulation run. The simulated synaptic strength resembles very closely the experimental one in all eight triplet stimulation paradigms.

As we can see from Figure 2, the plasticity results are inconsistent, because no obvious rule for potentiation and depression based on spike timings is evident. For instance, in the pre-5-post-5-pre and pre-10-post-10-pre scenarios, the saturated synaptic weight value W_∞ fluctuates around 0.0 and 0.05, respectively, whereas in the pre-5-post-15-pre scenario, W_∞ saturates at 0.23 (see Fig. 2A). In all post–pre–post stimulation paradigms, the synaptic weight changes are higher (see Fig. 2B). In the pre-10-post-10-pre paradigm where the spike timings are small (10 ms) and equal, the presynaptic and postsynaptic spikes add nonlinearly and produce a single high-peaked calcium spike (see Fig. 3B). This calcium pulse spends sufficient time above the 2 μM (veto) and 4 μM (potentiation) thresholds, thus yielding a high potentiation (P) response (see Fig. 3C). This high-peaked calcium response is followed by a prolonged decay back to zero due to the second presynaptic (dendritic) stimulation, which yields an additional calcium influx through the NMDA channels (see Fig. 3B). This calcium tail stays below the 2 μM and above the 0.6 μM thresholds for few tens of ms and triggers the depression signal (see Fig. 3D), which counteracts the effects of the potentiation signal (P)

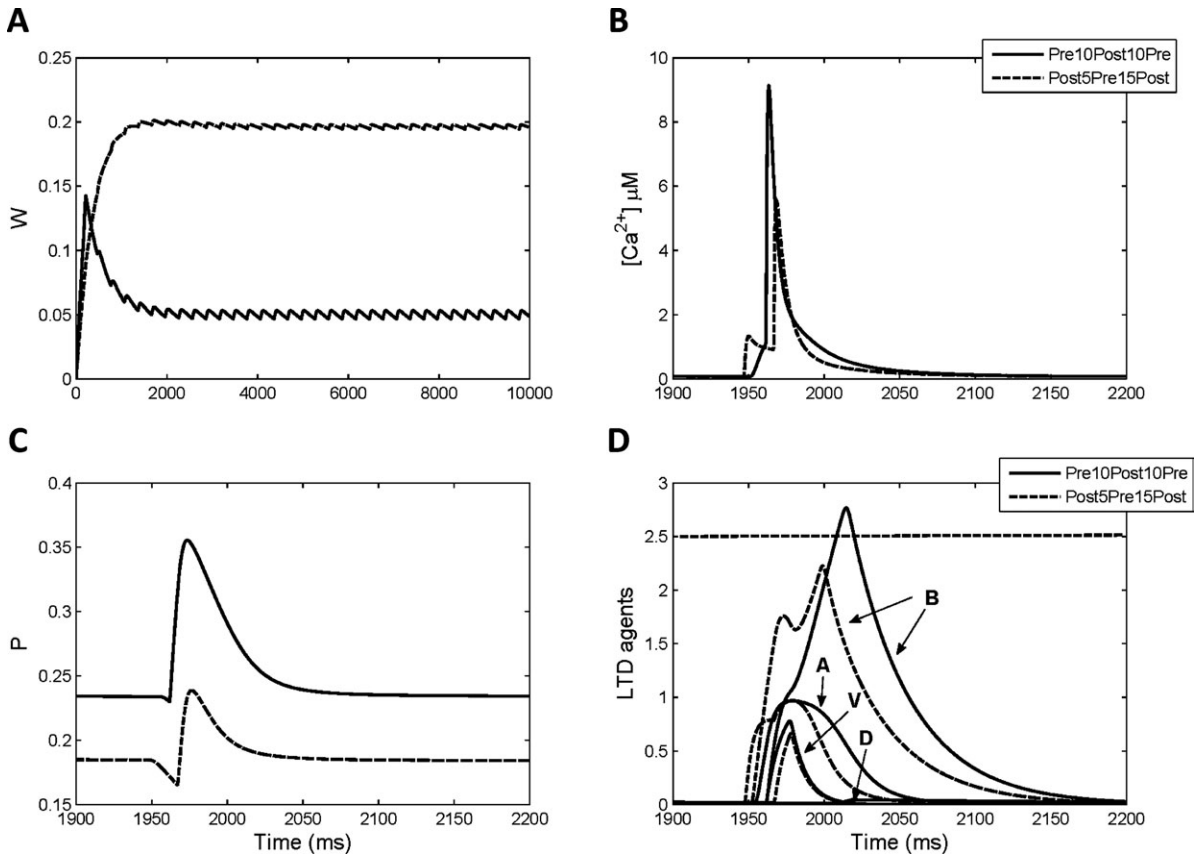

FIGURE 3. Comparison of (A) synaptic weight (*W*), (B) calcium concentration, (C) potentiation *P*, and (D) LTD agents (*A*, *B*, *V*, and *D*) time courses for two triplet stimulation protocols: pre-10-post-10-pre and post-5-pre-15-post in the absence of inhibition.

resulting in a low-synaptic strength (W) level (see Fig. 3A). In post-5-pre-15-post case, the calcium response is bimodal with the first low calcium peak resulting from the interaction of post-5-pre stimulation and second higher calcium peak resulting from the interaction of the pre-15-post stimulation (see Fig. 3B). The post–pre response is primarily due to calcium influx through VGCCs, whereas the pre–post one is due to calcium influx through the NMDA receptors. Because the calcium peak value is lower than in the pre-10-post-10-pre case, then the potentiation response (*P*) is lower (see Fig. 3C). The depression (*D*) response in this case is zero, because it is counteracted by the veto (*V*) signal, which prevents the *B* signal from exceeding the 2.5 threshold value and triggering depression (see Fig. 3D). Thus, depression (*D*) does not counteract the potentiation (*P*) effects as in the pre-10-post-10-pre case, and hence a much higher synaptic strength (*W*) change is observed (see Fig. 3A).

Triplets in the Presence of an 100 Hz Inhibitory Burst Bounded by the Onset and Offset of the Triplet Stimulation

Cutsuridis's (2011) study has shown that when a 100 Hz inhibitory burst bounded by the onset and offset of a doublet (a pair of spikes) stimulation, then the LTP and LTD peak values of the asymmetric STDP curve decrease. Here, I investigated the effects of a theta modulated high gamma (100 Hz) inhibitory spike train bounded by the onset and offset of the triplet stimulation (see Fig. 1D,E). As its strength (g_{GABA}) is gradually increasing, then the synaptic weight *W* decreases, as expected, in all pre–post–pre and post–pre–post stimulation paradigms (see Fig. 4). This is because the high-frequency inhibitory burst signal reduces the calcium influx through both the VGCC and the NMDA channels, thus resulting in the lower than normal calcium peak value, which does not cross the 4 μM threshold value, thus resulting in a low peak value for the potentiation *P* variable and an increased peak value for the depression *D* variable. The winner of the competition between *P* and *D* is, in most cases, the depression *D* (data not shown).

Triplets in the Presence of an Inhibitory Burst With Temporal Offset

Cutsuridis (2011) has shown that when a theta-modulated gamma inhibitory spike is present with the doublet excitatory stimulation and its onset coincides or partially overlaps with the onset of the postsynaptic stimulation, then the STDP shape undergoes a transition from asymmetry to symmetry. Here, I

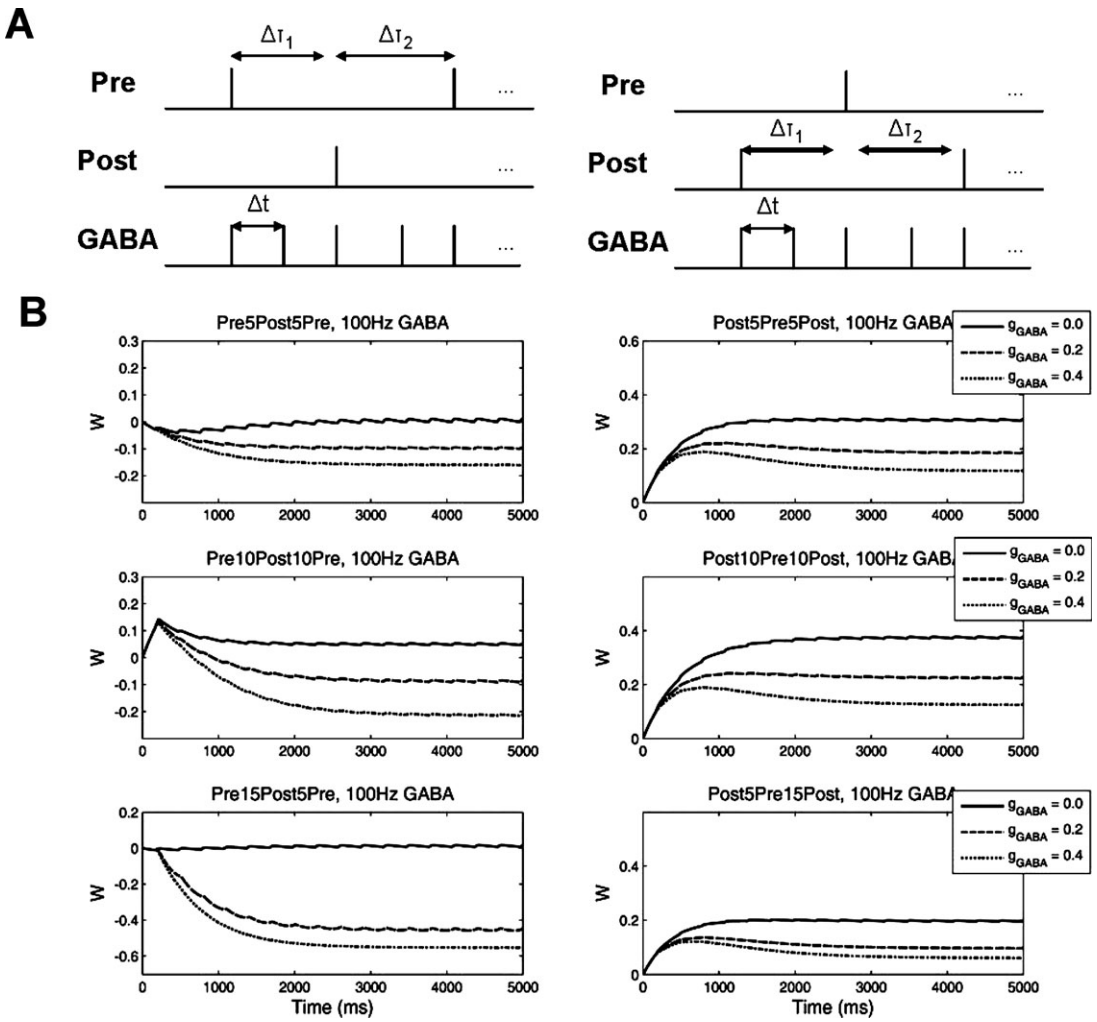

FIGURE 4. A: Model triplet stimulation protocols (pre–post–pre and post–pre–post) in the presence of an inhibitory burst with interspike interval of 10 ms (100 Hz). Both inhibitory burst and triplet stimulation were repeated every 300 ms. B: Comparison of synaptic weight (*W*) time courses for six different triplet (pre-5-post-5-pre, pre-10-post-10-pre, pre-15-post-5-pre, post-5-pre-5-post, post-10-pre-10-post, and post-5-pre-15-post) stimulation scenarios in the presence of an inhibitory burst with 10-ms interspike interval (100 Hz) bounded by the first and last spike of the triplet stimulation as a function of g_{GABA}.

investigated the effects of a theta-modulated high-gamma (100 Hz) inhibitory spike train present with the triplet excitatory stimulation and when its onset is either few milliseconds before or is partially overlapping with the onset of the first or last spike in the triplet stimulation. Then, depending of the stimulation paradigm employed, the synaptic weight *W* may decrease or increase as the inhibition strength increases (see Figs. 5 and Supporting Information Fig. S1). In Figures 5 and Supporting Information Fig. S1, each triplet stimulation paradigm (pre–post–pre or post–pre–post) with inhibition was repeated every 300 ms for about 5 s. In the pre-10-post-10-pre with inhibition scenario (see Fig. 5), where the inhibition precedes the triplet stimulation and its presentation offset aligns either with the onset of the first triplet spike or the second triplet spike, then as the strength of inhibition (g_{GABA}) increases, then the synaptic strength *W* decreases (see Figs. 5A,B). On the other hand, when the inhibition follows the triplet stimulation and its presentation onset aligns either with the onset of the second triplet spike or the last triplet spike, then as the strength of inhibition (g_{GABA}) increases, then the synaptic strength *W* increases (see Figs. 5C,D). In the post-5-pre-15-post with inhibition scenario (see Supporting Information Fig. S1), regardless of when the inhibition is introduced, as the strength of inhibition (g_{GABA}) increases, the synaptic strength *W* decreases.

In the pre-10-post-10-pre stimulation paradigm, when the onset of the inhibitory burst coincides with the onset of the last triplet spike [offset $= -(\Delta\tau_1 + \Delta\tau_2)$], an increase in *P* peak is evident as g_{GABA} increases (Fig. 6C). This is due to the high-calcium spike with the slow tail (see Fig. 6B), which prevents the depression component *B* to cross the 2.5 threshold value (see Fig. 6D), thus preventing the depression *D* signal to get activated (see Fig. 6D), which it would have counteracted the potentiation (*P*) signal. Thus, the synaptic weight change (*W*) is larger when g_{GABA} is nonzero.

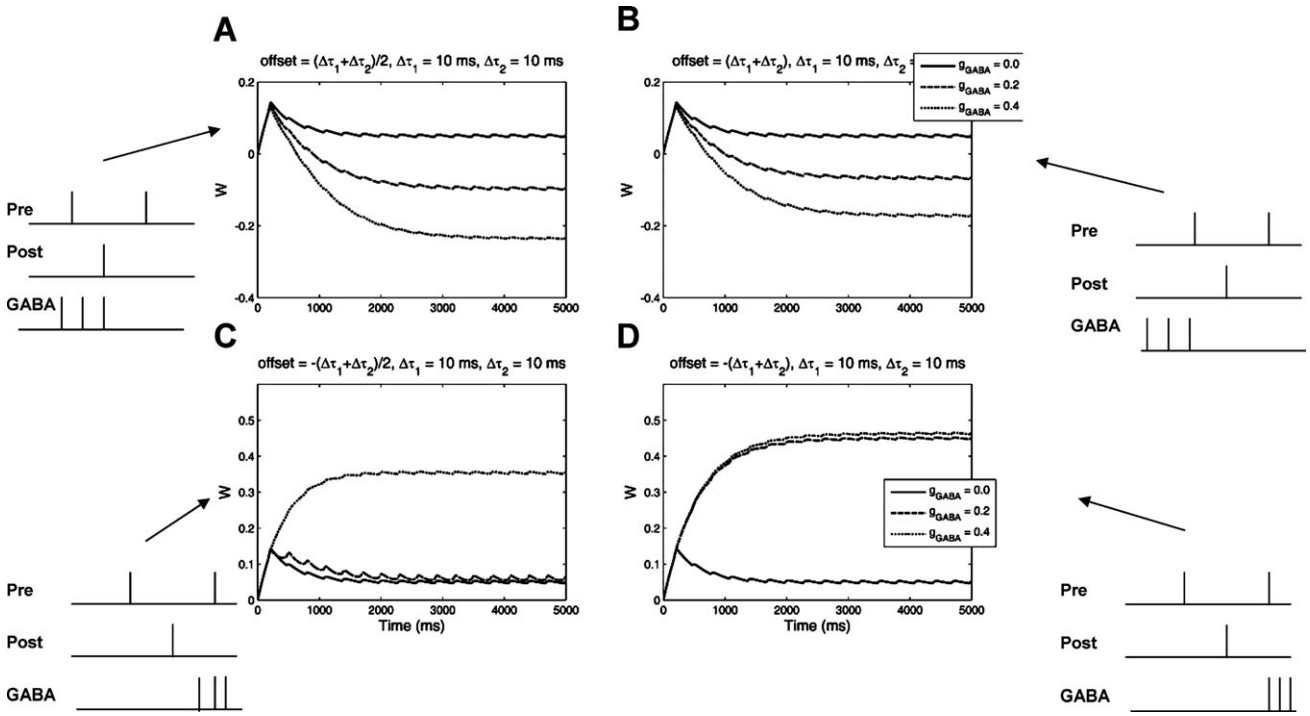

FIGURE 5. A–D: Comparison of synaptic weight (*W*) time courses for pre-10-post-10-pre stimulation scenario in the presence of an inhibitory burst with 10-ms interspike interval (100 Hz) with temporal offset as a function of g_{GABA}. Both GABA burst and triplet stimulation were repeated every 300 ms for about 5 s.

In the post-5-pre-15-post stimulation paradigm, when the onset of the inhibitory burst coincides with the onset of the last triplet spike [offset = $-(\Delta\tau_1 + \Delta\tau_2)$], a decrease in the *P* peak is evident as g_{GABA} increases (Supporting Information Fig. S2C). This is due to the progressive reduction of the calcium spike peak below the 4 μM threshold as g_{GABA} increases (Supporting Information Fig. S2B). The failure to cross the 4 μM threshold by the calcium spike results in the activation of a veto (*V*) response (Supporting Information Fig. S2D), which inhibits the initial but low-*D* response due to the low (barely above the 0.6 μM threshold) first calcium spike. So, the reduction in synaptic weight (see Supporting Information Fig. S2A) is due to a reduced *P* response and not due to an increased *D* response (Supporting Information Fig. S2C).

Direct comparison of the saturated synaptic weight (W_∞) value in the pre-10-post-10-pre stimulation paradigm with temporally offset inhibition [offset = $-(\Delta\tau_1 + \Delta\tau_2)$] as a function of inhibitory strength (g_{GABA}) and frequency of inhibition (50 Hz vs. 100 Hz) shows no synaptic weight change between the low gamma (50 Hz) and high gamma (100 Hz) cases (see Supporting Information Fig. S3).

Model Variations

The performance of the model was tested against a 5% variation of the calcium threshold basal parameter values (CmHC, CnHC, and θ_c in Table 2) in the pre-10-post-10-pre and post-5-pre-15-post stimulation paradigms in the presence of an 100-Hz inhibitory burst with temporal offset equal to $-(\Delta\tau_1 + \Delta\tau_2$; see Supporting Information Fig. S4). It is evident that the model's performance is robust enough under a 5% variation in its calcium dynamics.

DISCUSSION

What Have We Learned From the Model?

A two-compartment model of the CA1 pyramidal cell was presented to investigate how STDP in the dendrite of a CA1 pyramidal cell is induced by complex firing patterns such as triplets and how this plasticity is affected when the strength, frequency, and timing of inhibition co-present with the triplet stimulation is varied. The pyramidal cell model was an extension of the Cutsuridis's model (2011) to more complex inputs (triplets), which investigated the conditions under which the form of the STDP curve changes in the presence of inhibition (Nishiyama et al, 2000; Tsukada et al., 2005; Aihara et al., 2007). The present model's dynamics matched the experimentally observed triplet STDP results in the hippocampal cultured neurons (Wang et al., 2005; see Fig. 2 in this manuscript). With the parameter set unchanged, it computationally investigated how triplets and inhibition interact to shape the STDP when the strength, frequency, and timing of inhibition varied. The present model made a number of theoretical predictions:

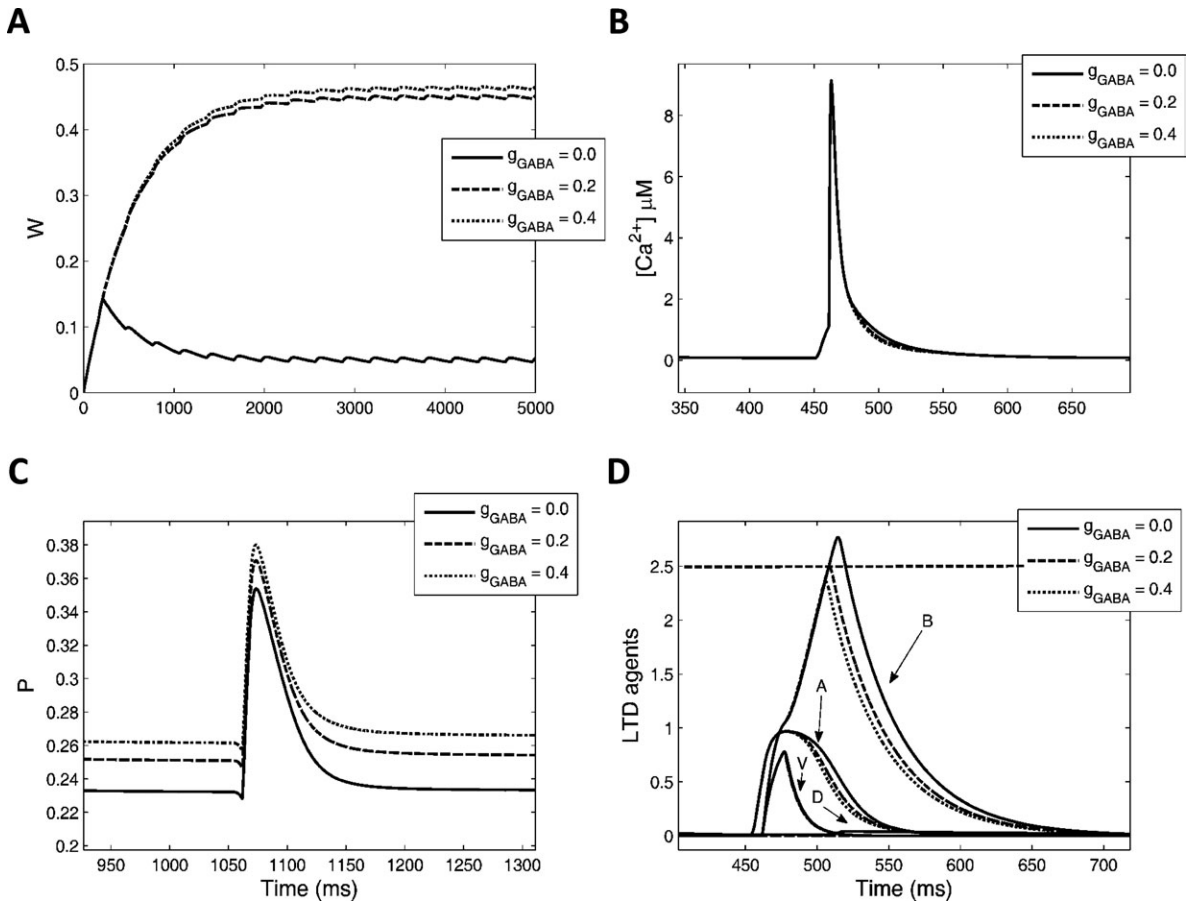

FIGURE 6. Time courses of (A) synaptic weight (*W*), (B) calcium concentration, (C) potentiation *P*, and (D) LTD agents (*A*, *B*, *V*, and *D*) for the pre-10-post-10-pre triplet stimulation protocol in the presence of a 100 Hz inhibitory burst with temporal offset as a function of g_{GABA}. Temporal offset was set to $-(\Delta\tau_1 + \Delta\tau_2)$, where $\Delta\tau_1 = 10$ ms and $\Delta\tau_2 = 10$ ms.

• The synaptic strength on a dendrite of a CA1 pyramidal cell is inversely proportional to the strength of inhibition impinging on it, when the presentation timing of inhibition coincides with the onset and offset of the triplet stimulation (see Fig. 4).
• When inhibition arrives either few milliseconds before or at the onset of the last spike in the pre–post–pre triplet stimulation, then the synapse is potentiated (see Fig. 5).
• Variability in the frequency of inhibition (50 vs. 100 Hz) co-present with the triplet stimulation shows no difference in synaptic strength value on the CA1 pyramidal cell dendrite (see Supporting Information Fig. S3).These theoretical predictions can easily be verified by experiments and that may lead to a better understanding of STDP in the CA1 pyramidal cell of the hippocampus.

Comparison With Other Models

Although few modeling studies have been published over the years where they attempted to investigate how triplets affect STDP, no modeling studies have been published with the exception of the author (Cutsuridis, 2011) who tried to study how pair excitation and theta-modulated inhibitory bursts interact to shape the STDP form. Mihalas (2011) recently introduced a simplified biochemical model of STDP where the heterogeneity of calcium concentrations of three calcium sources (VGCCs, NMDAR, and IP3R) in the nearby region of a spine was used as a STDP signal. The model was based on the biochemical cascades and assumption of spatial locations of four calcium-dependent enzymes: calcium/calmodulin-dependent protein kinase II located near NMDARs, calcineurin located near VGCCs, cyclic nucleotide phosphodiesterase (PDE) located near IP3Rs or NMDARs and adenylyl cyclase, located between VDCCs and NMDARs. The model reproduced the shape of STDP when pairs of spikes were used. The model predicted that if the cyclic nucleotide PDE is located near the IP_3 receptors, then the triplet experimental findings in hippocampal neuronal cultures were reproduced. If PDE is located near NMDAR, then the model behavior resembles that observed in cortical L2/3 slices. Pfister and Gerstner (2006) introduced a phenomenological model of STDP to fit the experimental triplet data from visual cortical slices and hippocampal cultures. The model predicted that in the presence of stochastic spike trains, the triplet learning rule maps to the

BCM learning rule. Later, Hennequin et al. (2010) used the Pfister and Gerstner model to investigate close-to-optimal information transmission. Shah et al. (2006) introduced a calcium-based plasticity model where the interaction of the triplet stimulation and the BPAP was quantitatively studied to explain the contradicting triplet experimental findings in visual cortical slices and hippocampal cultures. Cutsuridis (2011) is the only study and the basis of the present study where the effects of inhibition on spike timing-dependent synaptic plasticity were investigated quantitatively. Experimental evidence has shown that the form of STDP is location-dependent. More proximal to the soma of a CA1 pyramidal cell, the form of STDP is symmetric, whereas more distal to the soma is asymmetric (Nishiyama et al., 2000; Tsukada et al, 2005; Aihara et al., 2007). The Cutsuridis (2011) computational modeling study showed that this transition is due to inhibition under certain conditions such as its frequency, strength, and relative onset with pre–post excitatory stimulation.

Future Work

Several extensions to the basic idea of how inhibition affects STDP in the CA1 pyramidal cell deserve consideration. Work is underway to construct a more realistic model of a CA1 pyramidal neuron (Poirazi and Pissadaki, 2010). This model will include 17 different types of ions channels including L-, R-, and T-type Ca^{2+} currents. Wang et al. (2005) suggested that the unique determinant of potentiation and depression in the triplet stimulations may not be the L-type Ca^{2+} current, and perhaps other calcium mechanisms may play a more active role.

With such a realist model of the pyramidal neuron, I intent to study how STDP is modulated by more complex inputs such as presynaptic and postsynaptic bursts in the presence and absence of a theta-modulated inhibitory burst (Cutsuridis, 2012). Experimental evidence has shown that the synapses of CA1 pyramidal cells are surprisingly unreliable at signaling the arrival of single spikes to the postsynaptic neuron (Allen and Stevens, 1994). On the other hand, bursts are reliably signaled, because transmitter release is facilitated (Lisman, 1997). In the hippocampus, a single burst can produce long-term synaptic modifications (Lisman, 1997). Bursts of spikes in addition to increasing reliability of synaptic transmission, they have been shown to provide effective mechanisms for selective communication between neurons in a network (Izhikevitch et al., 2003).

Also, under certain experimental conditions, single APs in CA1 pyramidal cell distal dendrites attenuate and can fail to propagate into the proximal dendrites (Jarsky et al., 2005). This failure of AP propagation can be rescued during high-frequency bursts due to AP summation and the generation of dendritic calcium spikes (Letzkus et al., 2006). In addition, a number of studies have indicated a role of AP bursting in STDP (Kampa et al., 2006; Letzkus et al., 2006).

Previous work (Cutsuridis et al., 2009; Cutsuridis, 2010) has shown that the shape of the STDP curve undergoes a transition from asymmetry-to-symmetry based on the interspike interval of the burst when a presynaptic burst is paired with a postsynaptic spike or a presynaptic spike is paired with a postsynaptic burst. One of our future goals is to explore how a presynaptic burst interacts with a postsynaptic burst, how their interaction modulates STDP, and how STDP changes in the presence of a theta-modulated inhibition.

Finally, the effects of neighboring synapses on homosynaptic and heterosynaptic induction of LTP/LTD at the SR synapses of a CA1 pyramidal neuron will be computationally studied. These synapses can be localized on the same dendritic branch or on neighboring branches. The proximal, middle, and distal SR dendrites are bombarded by CA3 bursting Schaffer collateral inputs. Understanding the mechanisms under which adjacent synapses interact to generate homosynaptic and/or heteosynaptic LTP/LTD is of great importance to both single and network level modeling (Bi, 2002).

REFERENCES

Aihara T, Abiru Y, Yamazaki Y, Watanabe H, Fukushima Y, Tsukada M. 2007. The relation between spike-timing dependent plasticity and Ca^{2+} dynamics in the hippocampal CA1 network. Neuroscience 145:80–87.

Allen C, Stevens CF. 1994. An evaluation of causes for unreliability of synaptic transmission. Proc Natl Acad Sci USA 91:10380–10383.

Abarbanel HDI, Gibb L, Huerta R, Rabinovich MI. 2003. Biophysical model of synaptic plasticity dynamics. Biol Cybern 89:214–226.

Bear MF, Cooper LN, Ebner FF. 1987. A physiological basis for a theory of synapse modification. Science 237:42–48.

Bell CC, Han VZ, Sugawara Y, Grant K. 1997. Synaptic plasticity in a cerebellum-like structure depends on temporal order. Nature 387:278–281.

Bender VA, Bender KJ, Brasier DJ, Feldman DE. 2006. Two coincidence detectors for spike-timing-dependent plasticity in somatosensory cortex. J Neurosci 26:4166–4177.

Bi GQ. 2002. Spatiotemporal specificity of synaptic plasticity: Cellular rules and mechanisms. Biol Cybern 87:319–332.

Bi GQ, Poo MM. 1998. Synaptic modifications in cultured hippocampal neurons: Dependence on spike timing, synaptic strength, and postsynaptic cell type. J Neurosci 18:10464–10472.

Bland BH. 1986. The physiology and pharmacology of hippocampal formation of theta rhythms. Prog Neurobiol 26:1–54.

Bliss TV, Lomo T. 1970. Plasticity in a monosynaptic cortical pathway. J Physiol 207:61.

Bliss TV, Collingridge GL. 1993. A synaptic model of memory: Long-term potentiation in the hippocampus. Nature 361:31–39.

Buzsáki G. 2002. Theta oscillations in the hippocampus. Neuron 33:325–340.

Caporale N, Dan Y. 2009. Spike timing dependent plasticity: A Hebbian learning rule. Ann Rev Neurosci 31:25–46.

Cassenaer S, Laurent G. 2007. Hebbian STDP in mushroom bodies facilitates the synchronous flow of olfactory information in locusts. Nature 448:709–713.

Cho K, Aggleton JP, Brown MW, Bashir ZI. 2001. An experimental test of the role of postsynaptic calcium levels in determining synaptic strength using perirhinal cortex of rat. J Physiol (London) 532:459–466.

Cobb SR, Buhl EH, Halacy K, Paulsen O, Somogyi P. 1995. Synchronization of neuronal activity in hippocampus by individual GABAergic interneurons. Nature 378:75–77.

Cutsuridis V. 2012. Bursts shape the NMDA-R mediated spike timing dependent plasticity curve: Role of burst interspike interval and

GABA inhibition. Cognitive Neurodynamics, DOI: 10.1007/s11571-012-9205-1.
Cutsuridis V. 2011. GABA inhibition modulates NMDA-R mediated spike timing-dependent plasticity (STDP) in a biophysical model. Neural Networks 24:29–42.
Cutsuridis V, Cobb S, Graham BP. 2009. How bursts shape the STDP curve in the presence/absence of GABA inhibition. In Alippi C, Polycarpou M, Panayiotou C, Ellinas G, editors. LNCS 5768; Berlin Heidelberg: Springer-Verlag. pp 229–238.
Cutsuridis V. 2010. Action potential bursts modulate the NMDA-R mediated spike timing dependent plasticity in a biophysical model. In Diamantaras K, Duch W, Iliadis LS, editors. ICANN 2010, Part I, LNCS 6352; Berlin Heidelberg: Springer-Verlag. pp 107–116.
Debanne D, Gahwiler BH, Thompson SM. 1998. Long-term synaptic plasticity between pairs of individual CA3 pyramidal cells in rat hippocampal slice cultures. J Physiol 507:237–247.
Dudek SM, Bear MF. 1993. Bidirectional long-term modification of synaptic effectiveness in the adult and immature hippocampus. J Neurosci 13:2910–2918.
Dunwiddie T, Lynch G. 1978. Long-term potentiation and depression of synaptic responses in the rat hippocampus: Localization and frequency dependency. J Physiol 276:353–367.
Ermentrout B. 2002. Simulating, Analyzing and Animating Dynamical Systems. A Guide to XPPAUT for Researchers and Students. Philadelphia: SIAM.
Feldman DE. 2000. Timing-based LTP and LTD at vertical inputs to layer II/III pyramidal cells in rat barrel cortex. Neuron 27:45–56.
Froemke R, Dan Y. 2002. Spike timing dependent plasticity depends on dendritic location. Nature 416:221–225.
Froemke RC, Poo MM, Dan Y. 2005. Spike timing-dependent plasticity depends on dendritic location. Nature 434:221–225.
Froemke R, Tsay I, Raad M, Long J, Dan Y. 2006. Contribution of individual spikes in burst-induced long-term synaptic modification. J Neurophysiol 95:1620–1629.
Gall D, Prestori F, Sola E, D'Errico A, Roussel C, Forti L, Rossi R, D'Angelo E. 2005. Intracellular calcium regulation by burst discharge determines bidirectional long-term synaptic plasticity at the cerebellum input stage. J Neurosci 25:4813–4822.
Gloveli T, Kopell N, Dugladze T. 2010. Network activity patterns during hippocampal network oscillations in vitro. In Cutsuridis V, Graham BP, Cobb S, Vida I, editors. Hippocampal Microcircuits: A Computational Modeler's Resource Book (Springer Series in Computational Neuroscience 5). New York, USA: Springer Science + Business Media. pp 247–276.
Grover LM, Kim E, Cooke JD, Holmes WR. 2009. LTP in hippocampal area CA1 is induced by burst stimulation over a broad frequency range centered around delta. Learn Mem 16:69–81.
Hansel C, Artola A, Singer W. 1996. Different threshold levels of postsynaptic $[Ca^{2+}]_i$ have to be reached to induce LTP and LTD in neocortical pyramidal cells. J Physiol (Paris) 90:317–319.
Hansel C, Artola A, Singer W. 1997. Relation between dendritic Ca^{2+} levels and the polarity of synaptic long-term modifications in rat visual cortex neurons. Eur J Neurosci 9:2309–2322.
Harvey CD, Svoboda K. 2007. Locally dynamic synaptic learning rules in pyramidal neuron dendrites. Nature 450:1195–1200.
Hebb DO. 1949. The Organization of Behavior. New York: Wiley.
Hennequin G, Gerstner W, Pfister JP. 2010. STDP in Adaptive Neurons Gives Close-To-Optimal Information Transmission. Front Comput Neurosci. 4:143.
Hyman JM, Wyble BP, Goyal V, Rossi CA, Hasselmo ME. 2003. Stimulation in hippocampal region CA1 in behaving rats yields long-term potentiation when delivered to the peak of theta and long-term depression when delivered to the trough. J Neurosci 23:11725–11731.
Ismailov I, Kalikulov D, Inoue T, Friedlander MJ. 2004. The kinetic profile of intracellular calcium predicts long-term potentiation and long-term depression. J Neurosci 24:9847–9861.
Izhikevich EM, Desai NS, Walcott EC, Hoppensteadt FC. 2003. Bursts as a unit of neural information: Selective communication via resonance. TINS 26:161–167.
Jarsky T, Roxin A, Kath WL, Spruston N. 2005. Conditional dendritic spike propagation following distal synaptic activation of hippocampal CA1 pyramidal neurons. Nat Neurosci 8:1667–1676.
Kampa BM, Letzkus JJ, Stuart GJ. 2006. Requirement of dendritic calcium spikes for induction of spike-timing-dependent synaptic plasticity. J Physiol 574:283–290.
Karmarkar UR, Buonomano DV. 2002. A model of spike timing dependent plasticity: One or two coincidence detectors? J Neurosci 88:507–513.
Klausberger T. 2009. GABAergic interneurons targeting dendrites of pyramidal cells in the CA1 area of the hippocampus. Eur J Neurosci 30:947–957.
Klausberger T, Magill PJ, Marton LF, Roberts JD, Cobden PM, Buzsaki G, Somogyi P. 2003. Brain-state and cell-type-specific firing of hippocampal interneurons in vivo. Nature 421:844–848.
Klausberger T, Marton LF, Baude A, Roberts JD, Magill PJ, Somogyi P. 2004. Spike timing of dendrite-targeting bistratified cells during hippocampal network oscillations in vivo. Nat Neurosci 7:41–47.
Klausberger T, Somogyi P. 2008. Neuronal diversity and temporal dynamics: The unity of hippocampal circuit operations. Science 321:53–57.
Larson J, Lynch G. 1986. Induction of synaptic potentiation in hippocampus by patterned stimulation involves two events. Science 232:985–988.
Larson J, Lynch G. 1989. Theta pattern stimulation and the induction of LTP: The sequence at which synapses are stimulated determines the degree to which they potentiate. Brain Res 489:49–58.
Larson J, Wong D, Lynch G. 1986. Patterned stimulation at the theta frequency is optimal for the induction of hippocampal long-term potentiation. Brain Res 368:347–350.
Letzkus JJ, Kampa BM, Stuart GJ. 2006. Learning rules for spike timing-dependent plasticity depend on dendritic synapse location. J Neurosci 26:10420–10429.
Lisman J. 1989. A mechanism for the Hebb and the anti-Hebb processes underlying learning and memory. PNAS 86:9574–9578.
Lisman J. 1997. Bursts as a unit of neural information: Making unreliable synapses reliable. TINS 20:38–43.
Magee JC, Johnston D. 1997. A synaptically controlled, associative signal for Hebbian plasticity in hippocampal neurons. Science 275:209–213.
Markram H, Luebke J, Frotscher M, Sakmann B. 1997. Regulation of synaptic efficacy by coincidence of postsynaptic APs and EPSPs. Science 275:213–215.
Mayer ML, Westbrook GL, Guthrie BP. 1984. Voltage-dependent block by Mg^{2+} of NMDA responses in spinal cord neurons. Nature 309:261–263.
Mihalas S. 2011. Calcium messenger heterogeneity: a possible signal for spike timing-dependent plasticity. Front Comput Neurosci. 4:158.
Nowak L, Bregestovski P, Ascher P, Herbet A, Prochiantz A. 1984. Magnesium gates glutamate-activated channels in mouse central neurones. Nature 307:462–465.
Nishiyama M, Hong K, Mikoshiba K, Poo MM, Kato K. 2000. Calcium stores regulate the polarity and input specificity of synaptic modification. Nature 408:584–588.
Pavlides C, Greenstein YJ, Grudman M, Winson J. 1988. Long-term potentiation in the dentate gyrus is induced preferentially on the positive phase of theta-rhythm. Brain Res 439:383–387.
Pfister JP, Gerstner W. 2006. Triplets of spikes in a model of spike timing-dependent plasticity. J Neurosci 26:9673–9682.
Poirazi P, Pissadaki EK. 2010. The making of a detailed CA1 pyramidal neuron model. In Cutsuridis V, Graham BP, Cobb S, Vida I, editors. Hippocampal Microcircuits: A Computational Modeler's Resource Book (Springer Series in Computational Neuroscience 5). Springer Science + Business Media. pp 317–352.

Rose GM, Dunwiddie TV. 1986. Induction of hippocampal long-term potentiation using physiologically patterned stimulation. Neurosci Lett 69:244–248.

Rubin JE, Gerkin RC, Bi GQ, Chow CC. 2005. Calcium time course as a signal for spike-timing-dependent plasticity. J Neurophysiol 93:2600–2613.

Sabatini BL, Oertner TG, Svoboda K. 2001. Ca^{2+} signalling in dendritic spines. Curr Opin Neurobiol 33:439–452.

Seol GH, Ziburkus J, Huang SY, Song L, Kim IT, Takamiya K, Huganir RL, Lee HK, Kirkwood A. 2007. Neuromodulators control the polarity of spike timing dependent synaptic plasticity. Neuron 55:919–929.

Shah NT, Yeung LC, Cooper LN, Cai Y, Shouval HZ. 2006. A biophysical basis for the inter-spike interaction of spike-timing-dependent plasticity. Biol Cybern. 95:113–121.

Shouval HZ, Bear MF, Cooper LN. 2002. A unified model of NMDA receptor-dependent bidirectional synaptic plasticity. Proc Natl Acad Sci USA 99:10831–10836.

Sjostrom P, Turrigiano G, Nelson S. 2001. Rate, timing, and cooperativity jointly determine cortical synaptic plasticity. Neuron 32:1149–1164.

Stent GS. 1973. A physiological mechanism for Hebb's postulate of learning. PNAS 70:997–1001.

Tsukada M, Aihara T, Kobayashi Y, Shimazaki H. 2005. Spatial analysis of spike-timing-dependent LTP and LTD in the CA1 area of hippocampal slices using optical imaging. Hippocampus 15: 104–109.

Tzounopoulos T, Kim Y, Oertel D, Trussell LO. 2004. Cell-specific, spike timing-dependent plasticities in the dorsal cochlear nucleus. Nat Neurosci 7:719–725.

Wang HX, Gerkin RC, Nauen DW, Bi GQ. 2005. Coactivation and timing-dependent integration of synaptic potentiation and depression. Nat Neurosci 8:187–193.

White JA, Banks MI, Pearce RA, Kopell NJ. 2000. Networks of interneurons with fast and slow gamma-aminobutyric acid type A ($GABA_A$) kinetics provide substrate for mixed gamma–theta rhythm. PNAS 97:8128–8133.

Whittington MA, Traub RD, Jeffreys JGR. 1995. Synchronized oscillations in interneuron networks driven by metabotropic glutamate receptor activation. Nature 373:612–615.

Zhang L, Tao HW, Holt CE, Harris WA, Poo M. 1998. A critical window for cooperation and competition among developing retinotectal synapses. Nature 395:37–44.